RESEARCH ON MDO OF SHIP PROPULSION SHAFTING DYNAMICS CONSIDERING THE COUPLING EFFECT OF A PROPELLER-SHAFTING-HULL SYSTEM

Jinlin Liu
Zheng Gu *
Shuyong Liu
Naval University of Engineering, College of Power Engineering, Wuhan, China,

* Corresponding author: *guzhengzy@126.com (Zheng Gu)*

ABSTRACT

Dynamic designs for ship propulsion shafting can be categorised as complex multi-disciplinary coupling systems. The traditional single disciplinary optimisation design method has become a bottleneck, restricting the further improvement of shafting design. In this paper, taking a complex propulsion shafting as the object, a dynamic analysis model of the propeller-shafting-hull system was established. In order to analyse the coupling effect of propeller hydrodynamics on shafting dynamics, the propeller's hydrodynamic force in the wake flow field was calculated as the input for shafting alignment and vibration analysis. On this basis, the discipline decomposition and analysis of the subdisciplines in design of shafting dynamics were carried out. The coupling relationships between design variables in the subdisciplines were studied and the Multi-disciplinary Design Optimisation (MDO) framework of shafting dynamics was established. Finally, taking the hollowness of the shaft segments and the vertical displacement of bearings as design variables, combined with the optimal algorithm, the MDO of shafting dynamics, considering the coupling effect of the propeller-shafting-hull system, was realised. The results presented in this paper can provide a beneficial reference for improving the design quality of ship shafting.

Keywords: ship propulsion shafting, dynamic modelling, shafting alignment, shafting vibration, *multi-disciplinary design optimisation*

INTRODUCTION

Propulsion shafting is an important part of marine power plant. With the trend for upsizing and high-speed ships, the shafting structure is becoming more and more complex and its design process involves many different disciplines, such as structural mechanics, rotor dynamics and fluid mechanics, which belong to the design category of complex multi-disciplinary coupling systems [1]. Changes in design parameters and the coupling of dynamic factors, such as propeller hydrodynamic force and bearing support stiffness, will all affect the dynamic performance of shafting, to different degrees, influencing the reliability, concealment and other performance indexes of the whole power plant.

Alignment and vibration design are the core content of shafting dynamics analysis. At present, the relevant research on designing shafting dynamics optimisation is mainly carried out around these two points. For the optimisation of shafting alignment characteristics, recent research mainly focuses on optimisation by considering dynamic factors. Considering factors such as oil film stiffness, elastic deformation of the vibration isolator and dynamic stiffness, Yin [2] completed a comprehensive optimisation of alignment characteristics of a ship's flexible propulsion shafting by combining the Kirging response surface with a genetic algorithm. Using the established propeller-shafting-hull finite element model of a large crude oil carrier, Seo [3] analysed the influence of hull deformation, caused by draught change,

on shafting alignment; the results can provide guidance for the improvement of shafting alignment calculations. As for the optimisation of shafting vibration characteristics, current research is mainly focused on the new vibration absorber and the coupling vibration, under the influence of multiple factors. In [4], a dynamic vibration absorber with negative stiffness was proposed, which has the advantages of a low mass and small damping ratio; it has a remarkable effect on suppressing the longitudinal vibration of shafting under different operating modes. Huang [5] established an analysis model for the coupled transverse and torsional vibration of marine propulsion shafting, and further proposed an evaluation method for coupling vibration, considering the eccentricity of the cross section, damping coefficient and structural size.

In general, the optimisation design of shafting dynamics is mostly carried out from the perspective of a single discipline such as structure, alignment or vibration, and the coupling influence between multiple disciplines is rarely considered. This makes it difficult to acquire the optimal design results, which has become an immense obstacle, hindering the further improvement of shafting design quality.

The theory of Multi-disciplinary Design Optimisation (MDO) is a methodology that provides scientific guidance for the optimal design of a system by fully exploring and utilising the coupling effect and synergistic relationships between subdisciplines in complex systems, which is a powerful tool for solving engineering design problems. This theory was first presented in the field of aerospace; however, with continuous development, it has been extended to various walks of life, including ship design and propulsion. Gholinezhad [6] proposed a reliability-based MDO model for the design of an autonomous underwater vehicle and presented a method named the Sequential Optimisation and Reliability Assessment (SORA) to solve it. Lin [7] presented a methodology for the MDO of the life cycle benefit (LCB) of trimarans; the Monte Carlo Method was applied in the algorithm to achieve the optimisation. Nevertheless, for the application of MDO theory in the design of ship shafting, research is still in the exploratory stage. Liu [8] studied and established the MDO model for a marine motor driving shaft and realised the optimisation of alignment and vibration characteristics by changing the displacement of the stern bearing. The model is a short shaft that contains few design variables and the analysis method lacks consideration of the coupling effect between different disciplines.

By applying MDO theory to the dynamic design of ship shafting, we can acquire the optimal design scheme under the comprehensive consideration of the coupling effect between design variables. In this paper, by taking a complex propulsion shafting as the object, the dynamic analysis model of the propeller-shafting-hull system was established. On the basis of the disciplinary decomposition of shafting dynamics design and research on coupling relationships among subdisciplines, the MDO framework of shafting dynamics was proposed and an intelligent algorithm was used to realise the optimisation.

DYNAMIC ANALYSIS MODEL OF THE PROPELLER-SHAFTING-HULL SYSTEM

The hydrodynamic propeller force not only affects the shafting alignment state, but it is also the main excitation source of shafting vibration. Approximate methods were often used to calculate the hydrodynamic force as the input of analysis for shafting dynamics but the errors caused by approximate calculations did not guarantee the accuracy of the simulations. Hence, it is necessary to establish an integrated model of the propeller-shafting-hull system with a wake flow field model and use Computational Fluid Dynamics (CFD) methods to accurately calculate the hydrodynamic force. This considers the coupling effect of propeller hydrodynamics in the MDO framework of shafting dynamics.

INTEGRATED MODEL

Complex propulsion shafting mainly includes a propeller, three water lubricated bearings (including a front stern bearing, a rear stern bearing and a stern tube bearing), four intermediate bearings (numbered 1~4 from the stern to the bow of the shafting), a propeller shaft, a stern shaft, an intermediate shaft, flanges and couplings etc. The shafting is connected to the main engine by the gearbox and synchronous-self-shifting clutch. After simplification, the finite element analysis model of the shafting was established, as shown in Fig. 1.

With regard to the model in Fig. 1:

(1) Ignoring the coupling effect of vertical and horizontal stiffness (the subsequent modal analysis found that considering the coupling stiffness has little effect on shafting dynamics), a vertical and horizontal spring element was set at the fulcrums of each bearing and the stiffness values were reasonably set to simulate the bearing support [9]. Among them, the front and rear stern bearings adopted the multi-points model and the other bearings were supported by a single point;
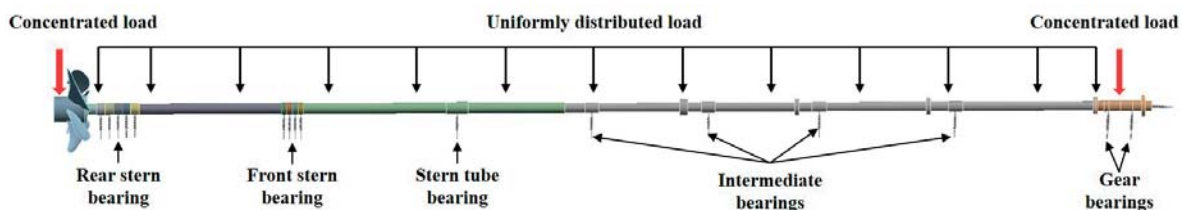

Fig. 1. Finite element analysis model of the propulsion shafting

(2) The gear shaft and two gear bearings were used to simulate the support in the gearbox and an axial spring was set at the output of the gearbox to simulate the thrust function of the bearings;

(3) The weight of the propeller and large gear was treated as concentrated load and the rest of the shaft segments were regarded as stepped shaft segments, applied as a uniformly distributed gravity load. The buoyancy coefficient of the propeller, propeller shaft and stern shaft was considered to be 0.87 and the material properties of various parts of the shafting are shown in Table 1;

(4) The reference coordinate system was designed as follows. Taking the geometric centre of the propeller as the coordinate origin, the inward vertical surface is the positive direction of the x axis; the upward direction is the positive direction of the y axis; the z axis is the axial direction, pointing to the bow is positive.

Tab. 1. Load and material properties of each part of the shafting

Parts	Young's modulus (N·m^{-2})	Poisson's ratio	Buoyancy coefficient	Density for calculation (kg·m^{-3})
Propeller	1.24 ×10^{11}	0.33	0.87	6525.0
Large gear	2.00 ×10^{11}	0.30	—	7850.0
Propeller shaft and stern shaft	2.00 ×10^{11}	0.30	0.87	6859.5
Other shaft segments	2.00 ×10^{11}	0.30	—	7850.0

A three-dimensional model of the hull was further established and assembled with the shafting to obtain the integrated model of the propeller-shafting-hull system, as shown in Fig. 2. It should be noted that, in order to improve the efficiency of the fluid simulation, propeller hydrodynamic force was calculated in the stack mould flow field of the hull, i.e. only the flow field below the waterline of the hull was considered. Therefore, only the hull model below the waterline was retained during modelling.
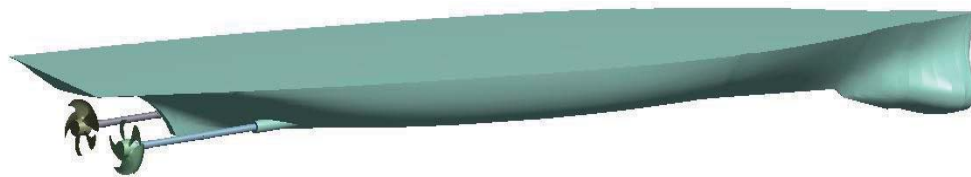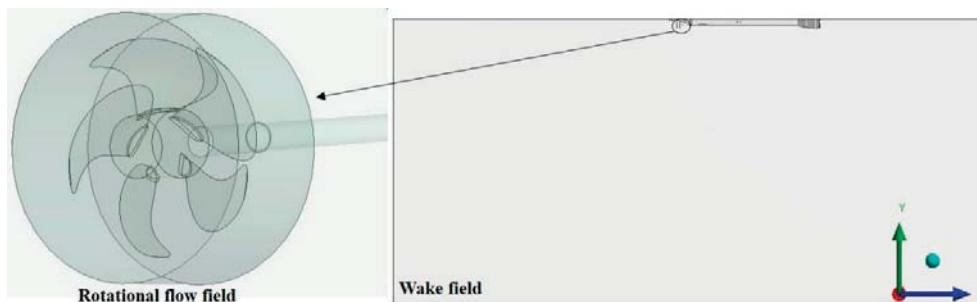
WATERSHED MODEL OF THE SHIP WAKE FIELD

A propeller's hydrodynamic force can be divided into surface force and bearing force, according to its transmission path; the bearing force is transmitted to the hull through shafting and is the main excitation source of shafting vibration. Relying on the integrated model in Fig. 2, the portside shafting was taken as an object to establish the watershed model of the wake field, as shown in Fig. 3.

The computational domain consists of two parts, one is the large wake field around the hull and the other is the small rotational flow field around the propeller. In order to ensure uniform incoming flow and consider the development of wake, the distance between the inlet of the large watershed and the bow of the ship is as long as the hull length, and the distance between the outlet and the stern of the ship is twice that of the hull length. The geometric centre of the cylindrical rotational flow field coincides with that of the propeller. Its diameter is 1.25 times the propeller diameter and its height is 1.05 times the propeller hub length.

SUBDISCIPLINE ANALYSIS

In MDO theory, disciplinary decomposition is the basis for optimal design. From the perspective of dynamic performance indexes, the design process of shafting dynamics was divided into three subdisciplines: statics, structural mechanics and rotor dynamics. Taking the dynamic analysis model as a platform, the design variables were selected after subdiscipline analysis.

Fig. 2. Integrated model of the propeller-shafting-hull system

Fig. 3. Watershed model of the ship wake field

STATICS ANALYSIS

In statics, the performance indexes relate to the dynamic characteristics of the shafting, mainly including the weight and size of shafting, which directly affects the torque transmission capacity and the loading capacity of the whole ship. The total weight of shafting can be estimated by Eq. (1) [10]:

$$G_t = \sum_{i=1}^{n} \rho_i V_i L_i g + G_a = \sum_{i=1}^{n} \rho_i \pi \left[\left(\frac{D_i}{2} \right)^2 - \left(\frac{d_i}{2} \right)^2 \right] L_i g + G_a(D) \quad \text{(1)}$$

where, ρ_i, V_i, L_i, D_i, and d_i represent the density, volume, length, outer diameter and inner diameter of the ith shaft segment, respectively; g is the gravitational acceleration; and $G_a(D)$ represents the weight of the auxiliary equipment of the shafting, positively related to the outer diameter of the shaft segment. In order to reduce the total weight of shafting, shafting mostly adopts a hollow design and the hollowness is used to express the hollow degree of the shaft segment, as shown in Eq. (2).

$$m_i = \frac{d_i}{D_i} \quad \text{(2)}$$

where m_i ($i=1,2,3$) is the hollowness of the ith shaft segment. The hollowness of each shaft segment can be adjusted within a certain range, while the outer diameter is directly related to the bearing selection and the design of relevant auxiliary equipment; it is difficult to change. Therefore, the value of hollowness is mainly adjusted by changing the inner diameter. The finite element model of shafting was transformed into hollow shafting by using a Boolean operation and the inner diameters of the propeller shaft, stern shaft and intermediate shaft were set as design variables. The whole process is shown in Fig. 4.
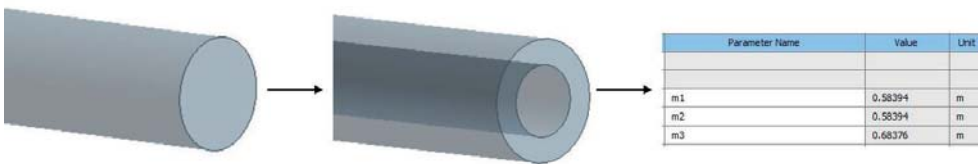

Fig. 4. The parameterisation of hollowness

STRUCTURAL MECHANICS ANALYSIS

The results of the structural mechanics analysis mainly show the relevant performance indexes of shafting alignment, including the load values of each bearing, the load difference between two adjacent bearings and the rotation angle of bearings etc. Poor alignment may lead to abnormal wear of the shafting and cause severe vibration [11]. Using the finite element method, the shafting is discretised into individual finite elements and the force and moment transfer equations between nodes are established. According to the actual force boundary conditions of shafting, the stress, rotation angle and reaction force can be calculated. The relationship equation of the reaction force at each node is:

$$R = K_e \delta_e \quad \text{(3)}$$

where K_e is the global stiffness matrix of the system, δ_e is the nodal displacement vector, and R is the nodal force vector. The nodal force corresponding to spring elements represents the bearing reaction force. After linear alignment calculations, the state parameters of each bearing are shown in Table 2.

Tab. 2. State parameters of each bearing under linear alignment

Name	Rotation angle (rad)	Bearing load (kN)	Specific pressure (N/mm²)	Allowable specific pressure (N/mm²)
Rear stern bearing	3.3827 e-6	398.33	0.11	0.80
Front stern bearing	-3.0143 e-5	102.39	0.07	0.80
Stern tube bearing	0.1569 e-6	161.05	0.15	0.30
Intermediate bearing 1#	-2.6387 e-5	100.03	0.17	0.80
Intermediate bearing 2#	3.2547 e-6	106.77	0.18	0.80
Intermediate bearing 3#	-1.2385 e-6	99.52	0.17	0.80
Intermediate bearing 4#	7.5265 e-7	123.67	0.21	0.80

According to Table 2, the rotation angle and specific pressure of each bearing are in the allowable range [12] but the load difference between front and rear stern bearings is too large, which will aggravate the wear of the rear stern bearing and the shaft segment it supports, causing service life reduction of the shafting components. Based on the watershed model of the ship wake field, the boundary conditions, such as incoming flow velocity and the rotating speed of the propeller, were set according to the design navigation condition of shafting (the RPM of the propeller is 150), and the propeller's hydrodynamic force was calculated by the CFD method. The time domain curves of thrust and torque of the propeller are shown in Fig. 5 and the pressure distribution on the surface of the propeller blades in the wake field was obtained, as shown in Fig. 6.
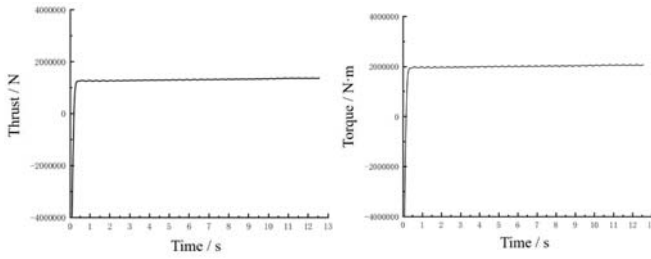
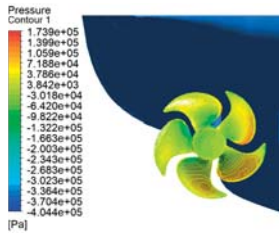*Fig. 5. Time domain curves of thrust and torque of the propeller*

Fig. 6. Pressure contour of propeller surface in the wake field
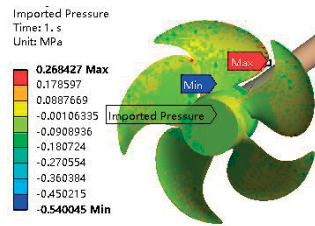

Fig. 7. Fluid-structure interaction

Setting the fluid-structure interface on the propeller surface, the propeller's hydrodynamic forces were applied to the propeller surface in the form of pressure (as shown in Fig. 7). Then, the alignment calculation was carried out again and the alignment results are listed in Table 3.

Tab. 3. State parameters of each bearing after reckoning in the propeller hydrodynamic force

Name	Rotation angle (rad)	Bearing load (kN)
Rear stern bearing	3.4541 e-6	258.61
Front stern bearing	-6.8015 e-5	118.64
Stern tube bearing	-6.5527 e-6	156.69
Intermediate bearing 1#	-6.7734 e-5	100.27
Intermediate bearing 2#	-3.4023 e-6	102.95
Intermediate bearing 3#	-5.0721 e-7	95.98
Intermediate bearing 4#	-6.8662 e-6	125.01

Comparing the data in Table 2 and Table 3, it can be seen that the load difference between front and rear stern bearings is reduced by 139.72 kN, after considering the hydrodynamic force, which indicates that the hydrodynamic force can effectively improve the working state of shafting during ship navigation. However, evidently, the load difference between front and rear stern bearings is still as high as 110.46 kN and so it is necessary to further adjust the vertical position of the bearings to optimise the alignment state. By setting the free length of the established spring elements as parameters, the parameterisation of the vertical position of the bearings can be realised. Additionally, the change of the hollowness of each shaft segment will also affect the shafting alignment by changing the mass. Consequently, the hollowness of shaft segments and the vertical displacement of bearings were selected as design variables in structural mechanics.

ROTOR DYNAMICS ANALYSIS

Influenced by the propeller excitation force and the pulsating excitation force of the main engine, shafting will inevitably generate a certain degree of vibration during its operation. An excessive vibration response is not conducive to the safe and stable operation of shafting and may induce large radiation noise, affecting the concealment of the whole ship. The complex propulsion shafting belongs to a multi-support rotor system, so the analysis of its vibration characteristics is a typical rotor dynamics problem. The rotor dynamics analysis equation based on the finite element method is:

$$[M]\{\ddot{x}\}+[C]\{\dot{x}\}+[K]\{x\}=\{F\} \tag{4}$$

where $[M]$, $[C]$ and $[K]$ represent the equivalent mass matrix, damping matrix and stiffness matrix at each node, respectively; $\{\ddot{x}\}$, $\{\dot{x}\}$ and $\{x\}$ represent the acceleration vector, velocity vector and displacement vector of each node, respectively; and $\{F\}$ represents the excitation force vector at each node. With regard to the long shafting with a gearbox, the gear meshing excitation force can be ignored and the excitation force mainly comes from the propeller.

According to Eq. (4), if the hollowness of each shaft segment changes, the shafting vibration response will be affected by the change of mass matrix. Furthermore, the vertical displacement of bearings shall be adjusted during the optimisation of alignment state and the load change of each bearing, after the change of vertical position, can be expressed as [13]:

$$\{R\}_y = \begin{Bmatrix} \Delta R_1 \\ \Delta R_2 \\ \vdots \\ \Delta R_n \end{Bmatrix} = \begin{bmatrix} a_{11} & a_{12} & \cdots & a_{1n} \\ a_{21} & a_{22} & \cdots & a_{2n} \\ \vdots & \vdots & & \vdots \\ a_{n1} & a_{n2} & \cdots & a_{nn} \end{bmatrix} \begin{Bmatrix} \Delta h_1 \\ \Delta h_2 \\ \vdots \\ \Delta h_n \end{Bmatrix} \tag{5}$$

where $\{R\}_y$ represents the variation vector of bearing load, ΔR_i is the load variation of the ith bearing, where i = 1, 2,…, n; a_{ij} is the bearing load influence coefficient, which represents the load variation of the jth bearing when the vertical displacement of the ith bearing changes by one unit length, where j = 1, 2,…, n; and Δh_i is the vertical displacement of the ith bearing. Considering the vertical displacement of the bearings, the coupling dynamic equation of the rotor system can be expressed by Eq. (6) [14]:

$$\begin{cases} [M]\{\ddot{Y}\}+[C_v]\{\dot{Y}-\dot{Y}_f\}+[K_v]\{Y-Y_f\}=\{F\}+\{R\}_y \\ [M_f]\{\ddot{Y}_f\}+[K_f]\{Y_f\}=[C_v]\{\dot{Y}-\dot{Y}_f\}+[K_v]\{Y-Y_f\} \end{cases} \tag{6}$$

where $[M]$ and $[M_f]$ are the rotor mass and the participating mass of vibration at each support, respectively; $[C_v]$ is the vertical damping coefficient of each bearing; $[K_v]$ and $[K_f]$ are the vertical oil film stiffness and the vertical structural

stiffness of each bearing, respectively; {F} is the external force on the support; {Y}, $\{\dot{Y}\}$ and $\{\ddot{Y}\}$ are the vertical vibration displacement, velocity and acceleration at each support, respectively; and $\{Y_f\}$, $\{\dot{Y}_f\}$ and $\{\ddot{Y}_f\}$ are the vibration displacement of the participating mass at each support, respectively. Eq. (6) shows that the change of vertical position of the bearings will also affect the vibration characteristics of the shafting.

In view of the theoretical analysis above, the sensitivity analysis method was used to further research the influence of the vertical displacement of the bearings on shafting vibration response. First of all, the modal analysis of the shafting was carried out to obtain the first six order modal shapes and frequencies within the highest excitation frequency, as shown in Fig. 8.
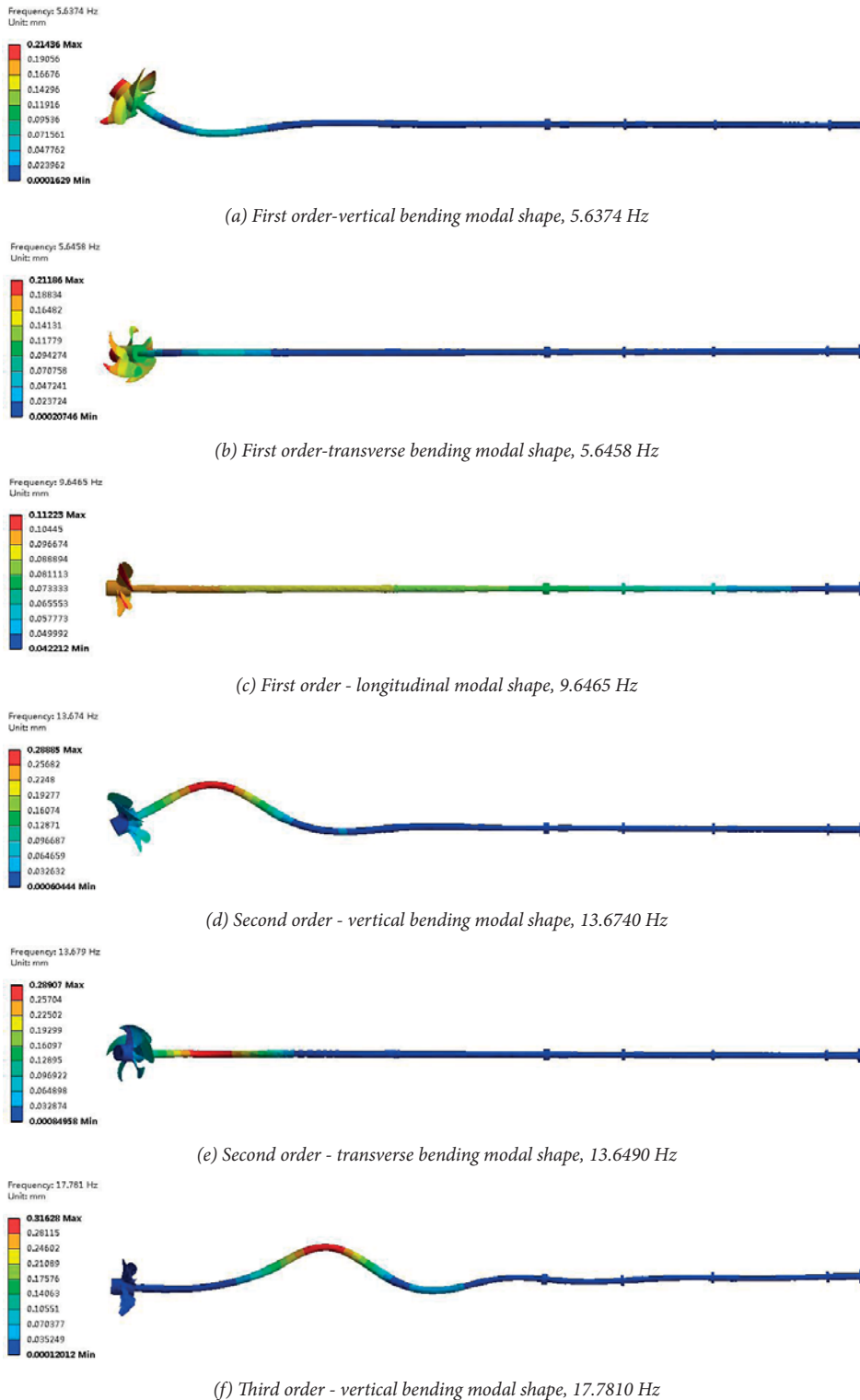

(a) First order-vertical bending modal shape, 5.6374 Hz

(b) First order-transverse bending modal shape, 5.6458 Hz

(c) First order - longitudinal modal shape, 9.6465 Hz

(d) Second order - vertical bending modal shape, 13.6740 Hz

(e) Second order - transverse bending modal shape, 13.6490 Hz

(f) Third order - vertical bending modal shape, 17.7810 Hz

Fig. 8. First six order modal analysis results of the shafting

According to the modal analysis results, a large vibration response emerges at the middle of the propeller shaft and stern shaft, so these two points were taken as the vibration monitoring points a and b, respectively. By transforming the propeller hydrodynamic force, calculated previously, into the resonant load [15] acting on the propeller, the amplitude-frequency response of the monitoring points can be analysed. As stern bearings are located outboard, and the sealing device is located at stern tube bearing, it is hard to adjust the vertical position for these three bearings at the stern of the shafting. Consequently, taking the vertical displacement of four intermediate bearings as variables, the sensitivity analysis results of the maximum amplitude of monitoring points, with respect to the vertical displacement, are shown in Fig. 9.
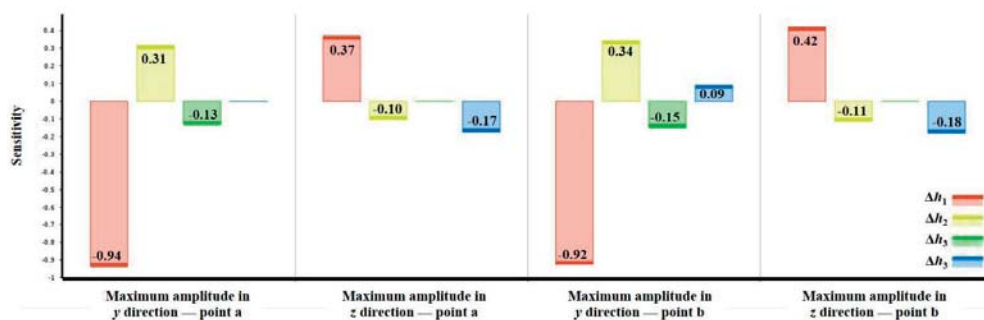

Fig. 9. Results of sensitivity analysis

In Fig. 9, $\Delta h_j\ (\ j =1, 2, 3, 4)$ represents the vertical displacement from No.1 to No.4 intermediate bearings. Due to limited space, only the sensitivity values of amplitudes in the y and z direction are given in the figure. It can be seen that the displacement of the No.1 intermediate bearing close to the stern of the shaft has a greater impact on the maximum amplitude, while the displacements of No.3 and No.4 intermediate bearings, with a long distance to the stern shaft, have smaller impacts. Moreover, the sensitivity of each bearing has negative values, so the vibration response of the shafting can be reduced by finding the optimal displacement values. For the above-mentioned analysis, in rotor dynamics, the hollowness of shaft segments and the vertical displacement of bearings can also be selected as design variables to optimise the dynamic characteristics of shafting.

COUPLING RELATIONSHIP AMONG SUBDISCIPLINES

In MDO theory, design variables can be divided into three types [16], as shown in Table 4.

Tab. 4. Classification and definition of design variables

Type	Definition
Discipline variable	Variables that only work within the scope of this discipline
Share variable	Variables shared by multiple disciplines, affecting the entire MDO system as input variables
Coupling variable	Output variables of discipline analysis as input variables of other disciplines

Apparently, according to the results of the subdiscipline analysis, the hollowness of shaft segments is obviously the share variable among the three subdisciplines. From the results of the rotor dynamics analysis, with the change of vertical position of the bearings, there is a coupling relationship of mutual input and output between the alignment state and vibration characteristics of the shafting. Hence, the vertical displacement of the bearings indicates the coupling variables between structural mechanics and rotor dynamics. The coupling relationship between three subdisciplines is shown in Fig. 10.
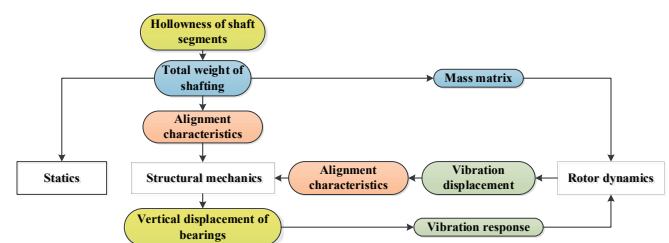

Fig. 10 Coupling relationship between subdisciplines

MDO FRAMEWORK FOR SHAFTING DYNAMICS

According to the analysis above, there is no hierarchical relationship among the subdisciplines but there is information interaction and a coupling relationship between structural mechanics and rotor dynamics. The whole design system of the shafting dynamics belongs to a non-hierarchical system, which means it is unnecessary to adopt a multi-level optimisation strategy to construct the MDO framework. Considering the lateral coupling relationship, the MDO framework for shafting dynamics was constructed by the Multi-Disciplinary Feasible (MDF) strategy.

MATHEMATICAL MODEL

According to MDF strategy, the mathematical model of the MDO framework was established, including optimisation objectives, system consistency constraints and the value range of design variables. Eq. (7) is the vector of design variables, including the hollowness of three shaft segments and the vertical displacement of four intermediate bearings; the MDO objective function of shafting dynamics was established, as shown in Eq. (8).

$$X = (m_1, m_2, m_3, \Delta h_1, \Delta h_2, \Delta h_3, \Delta h_4)^T \qquad (7)$$

$$\begin{cases} \min f(m_i, \Delta h_j, f_G, f_R, f_{\Delta R}, f_w, f_l) \\ f_G = \dfrac{G_A - G_A^*}{G_A^*}, \quad f_R = \dfrac{R_1 - R_1^*}{R_1^*}, \quad f_{\Delta R} = \dfrac{|R_1 - R_2| - |R_1^* - R_2^*|}{|R_1^* - R_2^*|} \\ f_w = \alpha_x \dfrac{d_{ax} - d_{ax}^*}{d_{ax}^*} + \alpha_x \dfrac{d_{bx} - d_{bx}^*}{d_{bx}^*} + \alpha_y \dfrac{d_{ay} - d_{ay}^*}{d_{ay}^*} + \alpha_y \dfrac{d_{by} - d_{by}^*}{d_{by}^*} \\ f_l = \alpha_z \dfrac{d_{az} - d_{az}^*}{d_{az}^*} + \alpha_z \dfrac{d_{bz} - d_{bz}^*}{d_{bz}^*} \\ m_1, m_2 \in [0.577, 0.606], \quad m_3 \in [0.675, 0.709], \quad \Delta h_j = [-5, 5] mm \end{cases} \qquad (8)$$

where f_G is the performance index function representing the total weight of shafting, G_A^*, G_A are the total weight before and after optimisation (kN), respectively; f_R and $f_{\Delta R}$ are the performance index functions representing the load of rear stern bearing and the reduction of load difference between front and rear stern bearings, respectively; R_1^*, R_2^* and R_1 R_2 are the load values of two stern bearings before and after optimisation (kN), respectively; f_w, f_l are the performance index functions representing the whirling vibration and longitudinal vibration of shafting; d_{ax}^*, d_{ay}^*, d_{by}^*, d_{by}^*, d_{ax}, d_{ay}, d_{bx}, and d_{by} are the maximum amplitudes in the x and y directions of the two vibration monitoring points, before and after optimisation (mm), repectively; d_{az}^*, d_{bz}^* 和 d_{az} and d_{bz} are the maximum amplitudes in the z direction of the two monitoring points before and after optimisation, respectively; and α_x, α_y and α_z are the weight coefficients, taken as 0.15, 0.35 and 0.50, respectively. To make optimisation results meet the relevant shafting design standards and specifications [17], the following consistency constraints were added to the mathematical model:

$$s.t. \quad 0.2 G_i \le R_i \le R_{i\max}$$
$$\sigma_{j\max} \le [\sigma]$$
$$\varphi_1 \le [\varphi] \qquad (9)$$
$$n_1 \ge 1.15 n_r, \quad n_1 = 9.55(2\pi f_1)$$
$$0.8 n_r \le n_z \le 1.2 n_r, \quad n_z = 9.55\left(\frac{2\pi f_1}{5}\right)$$

where $R_{i\max}$, R_i and G_i are the maximum allowable load, the load of the ith bearing and the total weight of the two adjacent shaft segments it spans, respectively; $\sigma_{j\max}$ and $[\sigma]$ are the maximum bending stress and allowable stress of the jth shaft segment (N/mm²), respectively; φ_1 and $[\varphi]$ are the rotational angle and allowable angle at the support of the rear stern bearing (rad), respectively; n_1 and f_1 are the critical speed (rpm) and the corresponding natural frequency (Hz) of the first order whirling vibration of shafting, respectively; n_r is the design working speed of shafting; and n_z is the subcritical speed of the propeller blades.

MDO FRAMEWORK

The MDO mathematical model has been established according to previous research. To obtain satisfactory optimisation results under the constraints in Eq. (9), it is essential to carry out multiple iterative calculations, in combination with the optimisation algorithm.

Since many design variables and optimisation objectives are contained in Eq. (8), the Non-dominated Sorting Genetic Algorithm-II (NSGA-II) was adopted as the optimisation algorithm. This algorithm supports multi-objective optimisation under multiple constraints and the elite individual reservation mechanism is added to the iteration process, which is conducive to finding the global optimal solution [18]. Interacting the algorithm with the parametric dynamic analysis model to obtain a large enough sample space of experimental points by the Design of Experiment (DOE) method [19, 20], the iterative optimisation calculation was performed to search for the optimal vector of design variables. The MDO framework of shafting dynamics, combined with the NSGA-II, is shown in Fig. 11.

MDO OF SHAFTING DYNAMICS

The parameters of NSGA-II were set as follows: the maximum number of iterations is 20, the maximum number of sample points per iteration is 61, the maximum allowable Pareto percentage is 70%, and the estimated sample space of the experimental points is 700. It can be seen from Fig. 11 that, in each iteration process, the parametric model is updated by the interaction of the sample data with the dynamic analysis results of each sample point, extracted to evaluate its fitness in the algorithm.

After iterative solving, the final vector of design variables obtained is X_{opt} = (0.598, 0.585, 0.684, 2.0, 0.9, -0.8, -1.4) ^{T}, which means that the hollowness of the propeller shaft, stern shaft and intermediate shaft were taken as 0.598, 0.585 and 0.684, respectively. The vertical position of No.1 and No.2 intermediate bearings were raised by 2.0 and 0.9 mm, respectively, while that of No.3 and No.4 intermediate bearings were lowered by 0.8 and 1.4 mm, respectively. Taking the hollowness of the stern shaft (m_2) and the vertical displacement of No.1 intermediate bearing (Δh_1) as examples, the optimisation process is shown in Fig. 12.
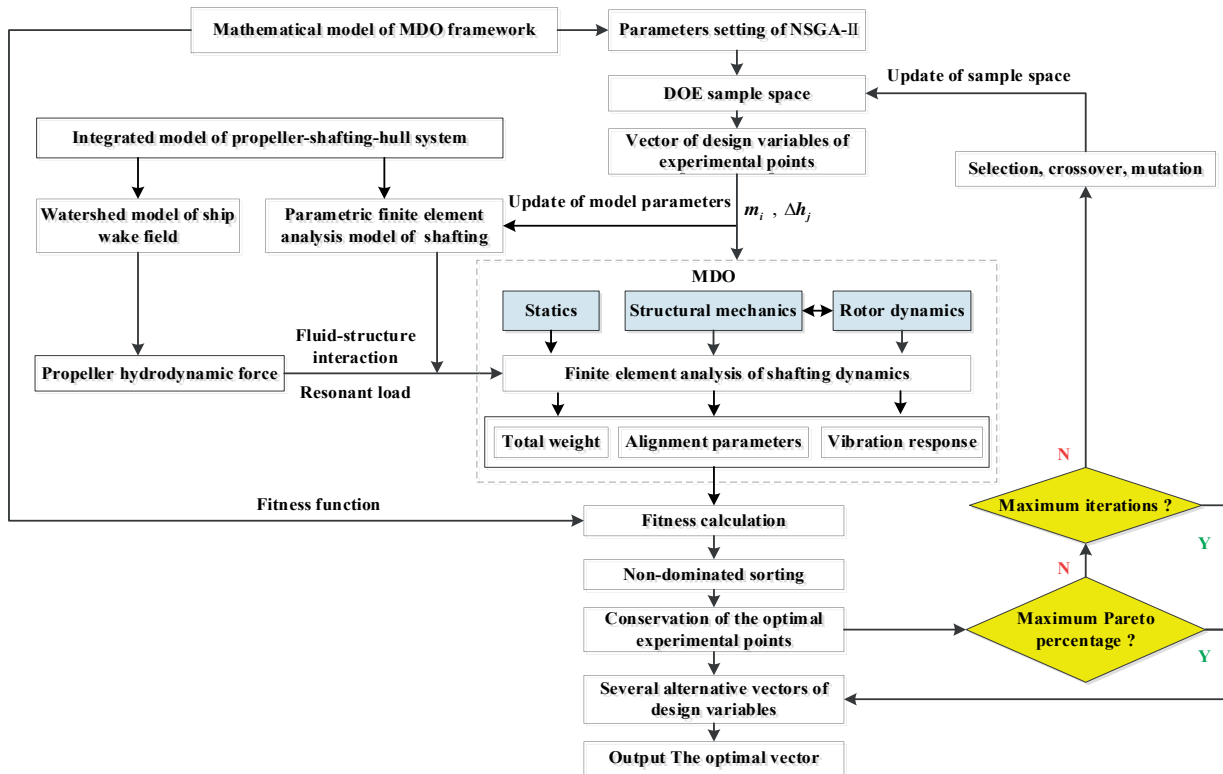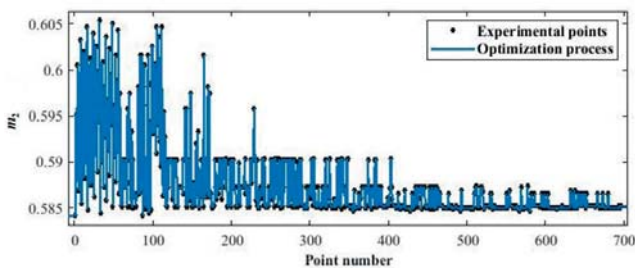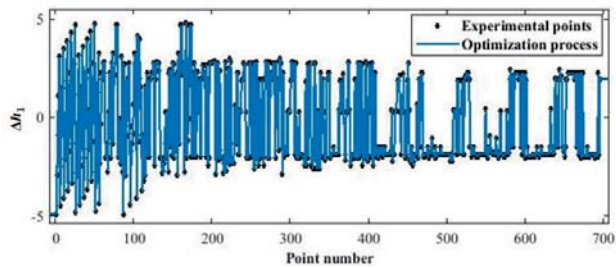
Fig. 11. MDO framework of shafting dynamics

(a) Optimisation process of m_2

(b) Optimisation process of Δh_1

Fig. 12. Optimisation process of design variables

Since the hollowness of the shaft segments changed, in order to verify whether the optimisation results meet the strength requirements of shafting, the strength of the dangerous cross sections of shafting must be checked. The maximum bending stress of shafting generally appears at the stern bearing [21], so the cross section where the rear stern bearing is supported

(No.1 cross section) and the cross sections where the diameter of the shaft changes at the head end (No.2 cross section) and tail end (No.3 cross section) of the rear stern bearing, were reckoned to be dangerous. The equations for the safety factors of these dangerous cross sections are available in the correlative shafting design standards [12], which will not be repeated here. Taking the yield strength of the material as 500 MPa and the tensile strength as 700 Mpa, the strength check results are shown in Table 5.

Tab. 5 Strength check results of dangerous cross sections

Dangerous cross sections	Composite average stress (N/mm²)	Composite alternating stress (N/mm²)	Safety factor	Allowable safety factor
No.1 cross section	78.80	40.66	3.49	2.00
No.2 cross section	78.80	39.45	3.53	2.00
No.3 cross section	112.41	40.96	2.82	2.00

According to Table 5, the safety factors of dangerous cross sections are greater than the allowable values, so the optimisation results of hollowness meet the strength requirements in shafting design. By updating the hollowness of shaft segments and the vertical position of intermediate bearings in the parametric model, the alignment calculation can be conducted again. The loads of each bearing, after MDO, are shown in Table 6.

Tab. 6. Load of each bearing after MDO

| Name	Vertical displacement (mm)	Bearing load (kN)
Rear stern bearing	0.0	219.25
Front stern bearing	0.0	137.97
Stern tube bearing	0.0	113.81
Intermediate bearing 1#	2.0	137.33
Intermediate bearing 2#	0.9	103.61
Intermediate bearing 3#	-0.8	94.94
Intermediate bearing 4#	-1.4	107.53

By comparing the data in Table 3 and Table 6, after MDO, the load of the rear stern bearing is reduced by 39.36 kN and the load difference between the front and rear stern bearings is reduced by 58.69 kN. The working state of the shafting is ameliorated. Furthermore, the amplitude-frequency response at the vibration monitoring points was analysed, after MDO. A comparison of the results of the vibration response, before and after optimisation, is given in Fig. 13 (the whirling vibration is represented in the y direction), and the maximum extracted amplitude is shown in Table 7.
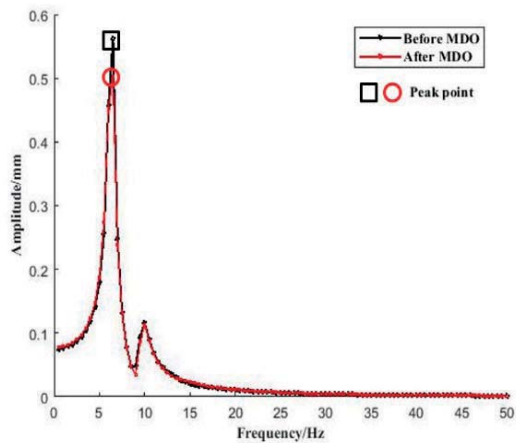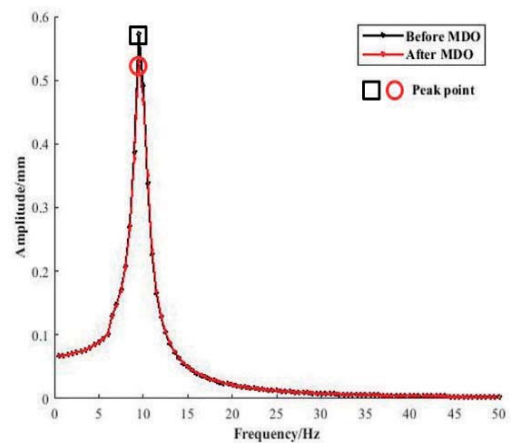

(a) Maximum amplitude (y direction) at point a
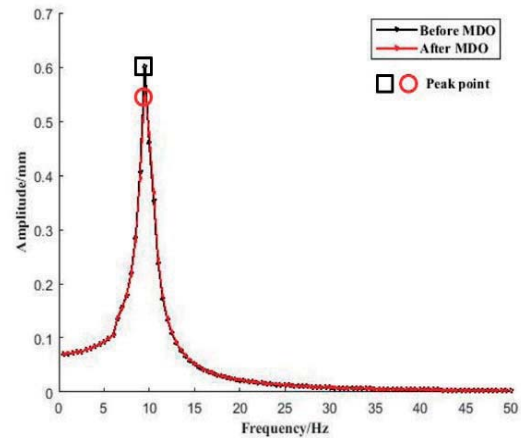
(b) Maximum amplitude (z direction) at point a
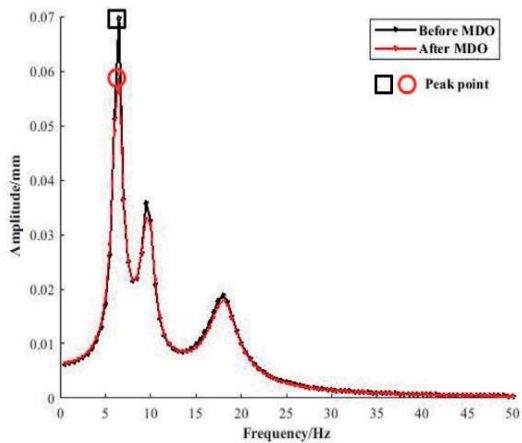
(c) Maximum amplitude (y direction) at point b

(d) Maximum amplitude (z direction) at point b

Fig. 13. Comparison of amplitude-frequency response at monitoring points before and after MDO

Tab. 7. Maximum amplitude of monitoring points before and after MDO (mm)

Direction	Point a		Point b	
	Before	After	Before	After
x direction	0.1051	0.1052	0.0378	0.0377
y direction	0.5615	0.5029	0.0699	0.0594
z direction	0.6009	0.5578	0.5724	0.5294

Combining Fig. 13 with the data in Table 7 shows that resonance peak points are near the modal frequency of each order. After optimisation, the amplitude in the x direction, at the propeller shaft and stern shaft, is basically unchanged, while the amplitude in the y direction and z direction decreases significantly. Overall, on the condition of meeting the design standards after MDO, the total weight of shafting is reduced, the alignment and vibration characteristics are improved, and the dynamic characteristics of the whole shafting is optimised.

CONCLUSIONS

Taking a complex propulsion shafting as a research object, this paper established an integrated model of a propeller-shafting-hull system and a watershed model of the wake field. Considering the coupling effect of propeller hydrodynamics, the design of shafting dynamics was divided into three subdisciplines: statics, structural mechanics and rotor dynamics. The design variables, including the hollowness of three shaft segments and the vertical displacement of four intermediate bearings, were selected after subdiscipline analysis and the coupling relationship between subdisciplines was studied. On this basis, the MDO framework of shafting dynamics was constructed and completed by combining it with the NSGA-II.

After MDO, with the total weight of shafting reduced, the load the of rear stern bearing is reduced by 39.36 kN, the load difference between the front and rear stern bearings is reduced by 58.69 kN and the vibration response of the shafting is also reduced.

The optimisation results show that the reliability, safety and concealment indexes of shafting operations are improved. The results of this research further enrich the design theory of ship propulsion shafting and provide a reference for promoting the design quality of shafting.

REFERENCES

1. J. Liu, F. Zeng, and J. Wu, Marine power plant. Huazhong University of Science and Technology Press, 2019.

2. H. Yin, J. Liu, L. Shi, F. Zeng, and S. Liu, 'Study on alignment characteristics of ship flexible propulsion shafting', Journal of Propulsion Technology, Vol. 43(04), pp. 401-409, 2021. doi: 10.13675/j.cnki.tjjs.200644.

3. C. Seo, B. Jeong, J-R. Kim, M. Song, J-H. Noh, and J. Lee, 'Determining the influence of ship hull deformations caused by draught change on shaft alignment application using FE analysis', Ocean Engineering, Vol. 210, 2020. 107488. doi: 10.1016/j.oceaneng.2020.107488.

4. X. Huang, Z. Su, and H. Hua, 'Application of a dynamic vibration absorber with negative stiffness for control of a marine shafting system', Ocean Engineering, Vol. 155, pp. 131-143, 2018. doi: 10.1016/j.oceaneng.2018.02.047.

5. Q. Huang, X. Yan, C. Zhang, and H. Zhu, 'Coupled transverse and torsional vibrations of the marine propeller shaft with multiple impact factors', Ocean Engineering, Vol. 178, pp. 48-58, 2019. doi: 10.1016/j.oceaneng.2019.02.071.

6. H. Gholinezhad and S.H. Torabi, 'Reliability-based multidisciplinary design optimisation of an underwater vehicle including cost analysis', Journal of Marine Science and Technology, Vol. 2, 2021. doi: 10.1007/s00773-021-00804-2.

7. L. Du, H. Hefazi, and P. Sahoo, 'Multidisciplinary Design Optimisation of Life Cycle Benefit of Trimarans Using Monte Carlo Method', Naval Engineers Journal, Vol. 131(3), pp. 79-90, 2011. doi: 10.1111/j.1559-3584.2010.00240.x.

8. J. Liu, G. Lai, H. Yin, F. Zeng, R. Zhou, and J. Lei, 'Research on multi-disciplinary design optimisation for marine motor driving shafting', Shipbuilding of China, Vol. 60(2), pp. 150-163, 2019. doi: 10.3969/j.issn.1000-4882.2019.02.015.

9. Y. Gao, 'Research on the theory and application of marine propulsion shafting alignment under dynamic factors'. Wuhan University of Technology, 2012.

10. G. Lai, J. Lei, J. Liu., S.Cao, H. Qin and F. Zeng, 'Numerical and experimental study on comprehensive optimisation for the KPIs of ship propulsion shafting design based on MDO', Ocean Engineering, Vol. 222, 108624, 2021. doi: 10.1016/j.oceaneng.2021.108624.

11. A. Ursolov, Y. Batrak, and W. Tarelko, 'Application of the optimisation methods to the search of marine propulsion shafting global equilibrium in running condition' Polish Maritime Research, vol.26, no.3, pp.172-180, 2019. doi: https://doi.org/10.2478/pomr-2019-0058.

12. CB/Z-338, 'Propulsion Shaft Alignment of Ship', 2005.

13. R. Zhou, 'The theoretic studies on the propulsion shafting alignment of ultra-large vessels', Wuhan University of Technology, 2005.

14. X. Pang, 'Study on characteristics of bearing load and coupling vibration in multi-support rotor system', Taiyuan University of Technology, 2011.

15. Z. Lei, J. Su, and H. Hua, 'Vibration and sound radiation analysis for a propeller-shaft-hullcoupled system in a catamaran SWATH ship', Journal of Vibration and Shock, Vol. 35(21), pp. 17-21, 2016. doi: 10.13465/j.cnki.jvs.2016.21.003.

16. H. Su, L. Gu, and C. Gong, 'Applying the disciplinary relation matrix to multidisciplinary design optimisation modelling and solving', Journal of Systems Engineering and Electronics, Vol. 28(4), pp. 703-716, 2017. doi: 10.21629/JSEE.2017.04.10.

17. CCS, 'Code for Naturalization and Construction of Steel Marine Vessels', Beijing: China Communications Press, 2015.

18. K. Deb, A. Pratap, S. Agarwal, and T. Meyarivan, 'A fast and elitist multiobjective genetic algorithm: NSGA-II', IEEE Transactions on Evolutionary Computation, Vol. 6(2), pp. 182-197, 2002. doi: 10.1109/4235.996017.

19. B. Zhang, P. Zhang, X. Guo, and F. Zeng, 'Multi-objective optimisation of marine diesel engine cooling system based on DOE-GA', Journal of Propulsion Technology, Vol. 41(11), pp. 2518-2529, 2020. doi: 10.13675/j.cnki.tjjs.200317.

20. K. Woloszyk and Y. Garbatov, 'Analysis of Ultimate Compressive Strength of Cracked Plates with the Use of DoE Techniques', Polish Maritime Research, vol. 27, no.3, pp. 109-120, 2020. doi: https://doi.org/10.2478/pomr-2020-0052.

21. Z. Liu, 'Research on intensity calculation and torsional vibration of marine shafting based on parameterization', Huazhong University of Science & Technology, 2012.